Polyelectrolyte Multilayers with Reversible Thermal Responsivity

Jad A. Jaber and Joseph B. Schlenoff*

Department of Chemistry and Biochemistry and Center for Materials Research and Technology (MARTECH), The Florida State University, Tallahassee, Florida 32306-4390

Received July 19, 2004; Revised Manuscript Received November 9, 2004

ABSTRACT: Thermally responsive polyelectrolyte multilayers were made from charged poly(*N*-isopropylacrylamide) (PNIPAM) copolymers. The temperature-dependent water content of the thin film, studied in situ using attenuated total reflectance Fourier transform infrared (ATR−FTIR) spectroscopy, revealed microscopic and macroscopic transitions at 33 and 45 °C, respectively. About seven water molecules per NIPAM repeat unit were found to be reversibly lost from, or recovered by, the film upon cycling over a temperature range of 10−55 °C. Assuming each ion pair represents a cross-link, swelling theory was used to translate these results into polymer−solvent interaction parameters and enthalpies of mixing for the various polymer components. The flux of a charged probe molecule, ferricyanide, through the NIPAM-rich multilayer was assessed with rotating disk electrode voltammetry. Thermally reversible modulation of ion transport was demonstrated.

Introduction

Poly(*N*-isopropylacrylamide) (PNIPAM) is a well studied polymer that exhibits interesting temperature-dependent aqueous solution properties.[1,2] It is soluble in water at low temperatures but becomes insoluble above the lower critical solution temperature (LCST).[3,4] At a LCST of 32−33 °C, the polymer undergoes a reversible volume phase transition, expelling water molecules originally solvating the isopropyl groups, enhancing their hydrophobic interaction and switching the polymer backbone conformation from a well hydrated coil to an insoluble globule.[5]

This stimulus-responsive material has found a variety of applications, for example, as column packing materials for temperature sensitive chromatography,[6] in substrates for cell culture,[7] for drug delivery systems[8] and in valves to control liquid transfer.[9] PNIPAM functionalized surfaces have been prepared using different grafting methods, including activated substrates and functionalized polymers,[10−13] electron beam irradiation,[14−16] photoinitiated grafting of functionalized polymer,[17−20] plasma-induced grafting,[21−23] and vapor-phase deposition by plasma polymerization.[24]

A simple alternative approach to the fabrication of PNIPAM thin films is via the layer-by-layer sequential adsorption technique,[25,26] which relies on multiple ion pairing interactions between charged groups to assemble blends, or complexes, of two or more polyelectrolytes. Thermoresponsive thin polymeric surfaces and stable hollow capsules of PNIPAM were produced in this manner.[27−29] However, their thermal characteristics exhibited only partially reversible behavior.[27]

In this paper, we describe the construction and characteristics of a thermoresponsive thin film, made with layer-by-layer sequential assembly, from ionically modified PNIPAM random copolymers (Figure 1): poly(allylamine hydrochloride)-*co*-poly(*N*-isopropylacrylamide), PAH-*co*-PNIPAM; and poly(styrene sulfonate)-*co*-poly(*N*-isopropyl acrylamide), PSS-*co*-PNIPAM. The thermosensitivity of these uniform "polyelectrolyte multilayers" (PEMUs) was evaluated using attenuated total reflectance Fourier transform infrared (ATR−FTIR) spectroscopy.[30−32] This proved to be a powerful in-situ technique for directly monitoring the amount of water within multilayers as a function of temperature, as well as revealing subtle changes in interactions between PNIPAM repeat units and water. Since many of the proposed applications of NIPAM composites rely on temperature control of membrane permeability, in drug release formulations for example, the permeability of multilayers was precisely determined by rotating disk electrode voltammetry (RDE). Transport of an electrochemically active probe molecule, potassium ferricyanide, through the thin film was substantially suppressed as temperature increased beyond 33 °C.

Figure 1. Structure of NIPAM copolymers used in this study.

Experimental Section

Reagents and Materials. Isopropylacrylamide, allylamine (98%), styrene sulfonic acid (sodium salt), 2-morpholinoethanesulfonic acid (MES), and potassium persulfate ($K_2S_2O_8$) were used as received from Sigma-Aldrich. Sodium chloride and tris(hydroxymethyl)aminomethane (Tris buffer) was from Fisher, and potassium ferricyanide was from Mallinckrodt. Deionized water (Barnstead, E-pure, Milli-Q) was used to prepare all aqueous solutions.

Copolymer Synthesis. PAH-*co*-PNIPAM. The copolymer (molecular weight 9.2×10^4, $M_w/M_n = 1.23$) was made via free radical polymerization of allylamine and isopropylacrylamide,[33] with a monomer feed ratio of 50:50 mol %. Allylamine monomer was transformed into a hydrochloride (white solid) by titrating it with excess concentrated HCl and then drying under vacuum for 18 h at 30 °C.

A solution of 2.34 g (0.025 mol) of allylammonium chloride, 2.83 g (0.025 mol) of isopropylacrylamide, and 0.021 g (0.4 mol %) of diethyl phosphite in 25 mL of *tert*-butyl alcohol, and a solution of 0.0165 g (0.2 mol %) of azoisobutyronitrile in 2.5 mL of chlorobenzene, were simultaneously added dropwise with stirring under N_2 to 5 mL of *tert*-butyl alcohol under

10.1021/ma0485235 CCC: $30.25
Published on Web 01/21/2005

reflux. The addition took 40 min and was followed by refluxing for 3 h. After cooling to 4 °C, the polymer was precipitated with ethyl acetate, and then dried at 80 °C for 18 h with a yield of 68%. Anal. Calcd (Atlantic Microlab) for PAH-*co*-PNIPAM, $(C_3H_8NCl)_{0.46}$-*co*-$(C_6H_{14}NO)_{0.54}$ (found): C, 52.3 (52.1); H, 9.2 (9.4); N, 13.6 (13.3); Cl, 17.2 (15.4).

PSS-*co*-PNIPAM. The copolymer (molecular weight 8.8×10^4, $M_w/M_n = 1.26$) was made via free radical polymerization of styrenesulfonate (sodium salt) and isopropylacrylamide, with a monomer feed ratio of 50:50 mol %. A solution of 2.83 g (0.025 mol) of isopropylacrylamide, 5.155 g (0.025 mol) of styrenesulfonates, sodium salt, and 0.014 g (0.1 mol %) of $K_2S_2O_8$, in 60 mL of distilled water, was heated ($T = 85$ °C) under N_2 for 24 h. The product was extensively dialyzed against distilled water using 14 000 molecular-weight-cutoff dialysis tubing; final yield was found to be 52%. Anal. Calcd for PSS-*co*-PNIPAM $(C_8H_7SO_3Na)_{0.45}$-*co*-$(C_6H_{14}NO)_{0.55}$, theory (found): C, 52.9 (53.1); H, 6.9 (7.1); N, 4.9 (5.1); S, 9.2 (9.0); Na, 6.6 (6.5).

Light Scattering. The hydrodynamic radius of the NIPAM copolymers was measured in solution using quasielastic light scattering, (QELS, Wyatt Technologies) equipped with temperature control. The measurements were carried out in a scintillation vial filled with either a 0.1 wt % solution of PAH-*co*-PNIPAM in 1.8 M NaCl and 25 mM MES buffer or 0.1 wt % solution PSS-*co*-PNIPAM in 0.2 M NaCl and 25 mM MES buffer. Buffer and salt solutions were filtered through 0.02 μm disposable filters (Whatman ANOTOP) and when the polymer was dissolved the whole solution was filtered again through 0.2 μm disposable filters. The temperature inside the vial was also monitored independently with a thermocouple.

Size exclusion chromatography−multiangle light scattering (SEC−MALS) measurements were performed at 25 °C using an Agilent 1100 series pump in series with a SEC column coupled to a DAWN-EOS light scattering detector (Wyatt Technologies) equipped with a He−Ne laser ($\lambda_0 = 690$ nm) and a Wyatt Optilab-DSP interferometric refractometer. SEC was performed with a 17 μm polymer column (300 mm × 7.5 mm, Tosoh Biosciences, covering the molar mass range 4×10^3 to 1×10^6 g mol^{-1}) in series with a TSK-GEL guard column. The mobile phase was 50 mM phosphate buffer (pH = 7.14) with 50 mM NaCl and 200 ppm of NaN_3. Injections were 50 μl of 0.5 wt % polymer solution. The sample specific refractive index increment, d*n*/d*c*, was determined offline using Wyatt's DNDC version 5.2. Data acquisition and handling was done using Astra 4.81.07. The DAWN-EOS instrument was calibrated with toluene. A 50 K dextran standard (Fluka), was used to normalize the fixed angle detectors on the DAWN-EOS and to verify performance of the SEC−MALS system (this standard was determined to be 5.06×10^4 g mol^{-1}; $M_w/M_n = 1.00$).

ATR—FTIR. The water content in multilayers was determined by ATR−FTIR ("ATR") spectroscopy.[30−34] ATR measurements were performed with a Nicolet Nexus 470 FTIR fitted with a 0.5 mL, temperature regulated, flow-through ATR assembly housing a 70 × 10 × 6 mm 45° germanium crystal (Specac Benchmark). The crystal was cleaned using 50:50 v/v ethanol/H_2O in saturated salt solution. Multilayer buildup on Ge was as follows: NIPAM containing polyelectrolyte multilayers, N−PEMU,[35] (PAH-*co*-PNIPAM/PSS-*co*-PNIPAM)$_{50}$@0.2 M NaCl@pH 6.5,[36] or polyelectrolyte multilayers, PEMU,[36] (PAH/PSS)$_{250}$@0.2 M NaCl@pH 6.5, were deposited from 10 mM polymer solutions on the ATR crystal using a robotic platform and then fitted into the ATR. Between alternating exposures to the polyelectrolytes, there were three rinses in 10 mM MES buffer with no NaCl added. Rinse and polymer solutions were approximately 50 mL each. The deposition time for each layer was 5 min, and each rinse was done for 30 s. The multilayer coated crystal was then kept in MES buffer (0.025 M, pH = 6.5) throughout all experiments. All spectra were recorded with 32 scans, at 1 cm^{-1} resolution for the peak position experiment and 4 cm^{-1} for the water content experiment. Background was bare, dry germanium crystal. The mole ratio of water to sulfonate at various temperatures was determined from the area under the respective peaks (3400 cm^{-1} for H_2O, 1035 and 1084 cm^{-1}). To calibrate instrument response a 1.0 M solution of poly(styrenesulfonate) (mole ratio of water:sulfonate = 55.6) was passed over the uncoated crystal. Using the sulfonate signal as a convenient internal standard normalizes out differences in absolute absorbance intensities of water (or propyl groups) that result from changes in refractive indexes of the multilayer.[32]

A water circulator (Thermo Haake) controlled the temperature of the flow cell over the range 10−50 °C (±0.1 °C). Temperature was also monitored using a thermocouple in contact with the surface of the crystal. The response of the NIPAM fraction to temperature was monitored using the amide II peak shift at 1550 cm^{-1}. Multilayer thicknesses on the Ge crystal were measured with a profilometer (P-15 Tencor instruments) at step edges (scratches).

RDE Voltammetry. Electrochemical measurements were done using a 100 mL electrochemical cell equipped with a water jacket, controlled over a temperature range of 10−50 °C (±0.1 °C), a platinum counter electrode, and a KCl-saturated calomel electrode (SCE), against which all potentials are quoted.[37] The working electrode was a rotating (at 1000 rpm) platinum disk (RDE, from Pine Instruments), 8 mm diameter, mounted in a Pine ASR2 rotator and speed controller. All solutions were deoxygenated with argon prior to electrochemical measurements. Potential ramps were generated by an EG&G Princeton Applied Research 273 potentiostat interfaced to a computer. The electrode was polished with 0.05-μm alumina (Buehler), sonicated, and rinsed in water. The electrode was further sonicated in a mercaptoethanesulfonic acid solution before multilayer deposition to maintain a negatively charged surface. Adsorption of N−PEMUE, (PAH-*co*-PNIPAM/PSS-*co*-PNIPAM)$_{18}$(PAH-*co*-PNIPAM)@0.2 M NaCl@pH 9 or PEMUE, (PAH/PSS)$_{18}$(PAH)@0.2 M NaCl@pH 9, onto the rotating disk electrode RDE was done at 300 rpm from 10 mM polymer solutions in Tris buffer (pH = 9) with the aid of a robot (StratoSequence V, nanoStrata Inc.). Potassium ferricyanide solutions were prepared in MES buffer (0.025 M, pH = 6.5). The concentration of redox probes was 1 mM with a supporting electrolyte concentration of 2.0 M NaCl. Flux measurements were obtained using steady-state RDE voltammetry.[38] Throughout all electrochemical runs, solution temperature was monitored using a thermocouple. Thicknesses on Pt were estimated by depositing multilayers on silicon wafers under the same conditions and measuring their thicknesses with a Gaertner Scientific L116S autogain ellipsometer with 632.8 nm radiation at 70° incident angle and multilayer refractive index of 1.54.

Prior to all experiments, a multilayer was allowed to anneal for 2 h in Tris buffer solution (0.025 M, pH = 9) at 40 °C and then stored in the same solution at room temperature.

Results and Discussion

The response of NIPAM membranes to temperature depends on the amount of NIPAM present and also on the ability of the hydrophobic moieties to interact and collapse upon transition.[1] In this system, NIPAM copolymers were ionically modified with PAH and PSS, which are known to have strong ion pairing interactions, producing multilayers that are resistant to swelling and rearrangement.[39−41] This strong ion pairing also drives blending at the molecular level and prevents phase separation on heating cycles. The degrees of freedom for NIPAM in a multilayer will be substantially reduced as compared to solution. With the high degree of interpenetration present in a multilayer, and the random nature of the copolymers, thermoresponsivity is still expected to manifest itself when isopropyl groups on the same or different copolymer molecules associate due to hydrophobic interactions, albeit to a much lower extent compared to what is observed in solution. Such behavior was noted for a charged, cross-linked NIPAM copolymer gel,[42] where the degree of shrinking or collapsing decreased as the cross-linker concentration

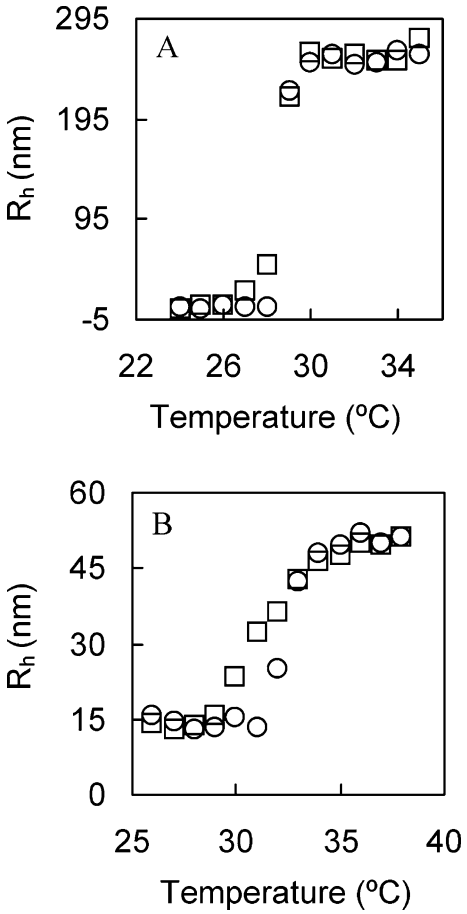

Figure 2. Increase in hydrodynamic radius as a function of temperature. (A) Circles and squares are, respectively, the heating and cooling cycles of PAH-*co*-PNIPAM (1.8 M NaCl, 0.025 M MES, pH = 6.5, R_h = 8.0 nm at 25 °C). (B) Circles and squares are the respective heating and cooling cycles of PSS-*co*-PNIPAM (0.2 M NaCl, 0.025 M MES, pH = 6.5, R_h = 14.0 nm at 25 °C).

increased, paralleled by a lower enthalpy of dissociation of hydrophobic interactions than that observed for PNIPAM in solution.[42]

Charged NIPAM Copolymers. The chemical environment of the polymer strongly affects its LCST. In general, incorporation of hydrophobic monomers lowers the LCST and hydrophilic monomers increase LCST.[43−45] Charge can also affect the transition temperature: it was demonstrated that, in the presence of ionized carboxyl side groups, the LCST for certain polypeptide solutions will increase.[46] In the case of charged NIPAM copolymers, a similar trend was observed, and the phase transition was completely suppressed at high content of ionic groups.[43] Increasing the ionic strength of the bathing solution counteracts the effect of polymer charge and recovers the copolymer thermoresponsivity.[43]

When the thermoresponsivity of PAH-*co*-PNIPAM was studied in solution (0.025 mM MES, pH = 6.5) using QELS, no transitions in the effective hydrodynamic radius (R_h) over the temperature range 25−85 °C were observed when the salt concentration was less than 0.50 M NaCl.

At 0.60 M NaCl the transition occurred around 75 °C and decreased to 30 °C as the ionic strength increased to 1.8 M accompanied by an increase in R_h (Figure 2) indicating (reversible) aggregation of PAH-*co*-PNIPAM chains. PSS-*co*-PNIPAM showed similar trends, having an elevated LCST at low salt concentration, but electrostatic interactions were suppressed at a much lower ionic strength of 0.2 M NaCl, at which point the transition temperature was 34 °C. The inflection point of the curve is considered to be the LCST. In both cases, increasing the ionic strength of solution will increase its osmotic pressure,[47] which favors the extraction of water molecules hydrating the copolymer chains into bulk water, in addition to decreasing the effective charge density down to a critical value,[43] below which the temperature induced transition is restored. The polymer−polymer affinity of PSS-*co*-PNIPAM at high temperatures is stronger than that of PAH-*co*-PNIPAM (which is more hydrophilic and with a higher charge density, p$K_a \sim 9$[48,49]) due to the hydrophobic aromatic groups of PSS. Thus, polymer collapse and hydrophobic interactions in PSS-*co*-PNIPAM are facilitated at lower salt concentrations.

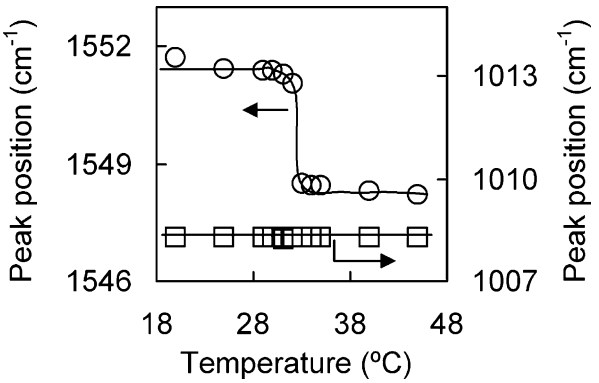

Figure 3. Effect of temperature on the peak position of the amide II band in N−PEMU, (PAH-*co*-PNIPAM/PSS-*co*-PNIPAM)$_{50}$@0.2 M NaCl@pH 6.5. Circles and squares correspond to the position of amide II and sulfonate peaks, respectively. The transition was sharp, occurring between 32 and 33 °C.

Thermoresponsivity of N—PEMU. ATR−FTIR is very effective in probing film/liquid interfaces—it provides a wealth of information regarding the local environment[50] and conformational backbone changes within N−PEMU. The IR spectra of NIPAM copolymers show a prominent peak in the region 1550−1450 cm^{-1}, assigned to N−H bending and C−N stretching modes. This amide II band is conformationally sensitive and can be used to report changes in the environment of the isopropyl groups during phase transitions.[50]

N−PEMU was deposited on the surface of a Ge crystal used for ATR−FTIR. The thickness of the N−PEMU (4.6 μm, dry) was such that the evanescent wave (0.6 μm at 1000 cm^{-1} for the system described; see Supporting Information for an estimate) emanating from the ATR crystal was contained completely within N−PEMU. As temperature increased to about 33 °C, hydrophobic interactions induced the association of isopropyl groups, and a sudden shift toward lower wavenumber was evident (Figure 3).

The sulfonate peak around 1010 cm^{-1}, used as an accurate internal standard,[32] was found to be independent of temperature. Thus, the observed shift in the peak position of amide II band cannot be attributed to changes in the refractive index of the multilayer when the temperature was changed but rather to a true sharp phase transition involving associated isopropyl groups.

A typical cross-linked NIPAM hydrogel is swollen, hydrated, and hydrophilic below the LCST but becomes collapsed, dehydrated, and hydrophobic above that temperature.[52] To investigate whether the multilayer

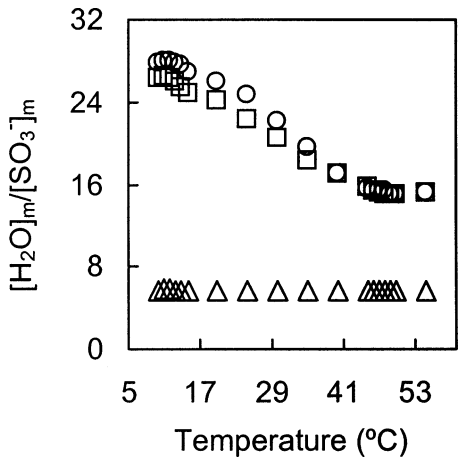

Figure 4. Mole ratio of water to sulfonate vs temperature. Circles and squares correspond to water content in N−PEMU, (PAH-*co*-PNIPAM/PSS-*co*-PNIPAM)$_{50}$@0.2 M NaCl@pH 6.5, during respective heating and cooling cycles. Triangles correspond to loss of water from PEMU, (PAH/PSS)$_{250}$@0.2 M NaCl@pH 6.5.

responded similarly, the amount of water present in the multilayer was determined at different temperatures (Figure 4). When compared to the control PEMU,[41] N−PEMU has approximately 5 times more water due to the presence of hydrated NIPAM groups and when the temperature increased, it lost almost 50% of its water while PEMU lost less than 10%.

Although loss of water from both multilayers was observed, thermoreversibility was seen only for N−PEMU. Upon cooling, N−PEMU was found to recover roughly the same amount of water lost at higher temperatures. However, in the case of PEMU, even after 2 weeks at room temperature, the small amount of water lost was not recovered (data not shown).

Comparing Figures 3 and 4, it is clear that the isopropyl phase transition (Figure 3) and the expulsion of water (volume transition) occur over different temperature ranges, in contrast to behavior recorded for a cross-linked neutral NIPAM gel.[53] In the latter case, dehydrated isopropyl groups interact and collapse once the LCST is reached i.e., at the same temperature when water molecules hydrating the NIPAM segments are lost, causing the gel to shrink concurrently.[53] However in the case of N−PEMU, loss of water molecules (volume transition) is continuous (second order) and occurs over a wider temperature range of 10−45 °C while hydrophobic association (phase transition) is discontinuous (first order) and occurs at 33 °C.

The individual polymer charges within a PEMU are generally well matched (intrinsic charge compensation) with minimal participation of salt counterions (extrinsic compensation).[32] In the case of exact polymer charge matching, in a PEMU that contains NIPAM, one would expect no long-range electrostatic repulsion effects, and thus no perturbation of the expected narrow volume transition. A small amount of extrinsic charge impacts volume transitions. For example, a small amount of charge introduced into cross-linked PNIPAM gels[42] shifted the temperature for volume transitions significantly. In these gels, the difference between volume and first-order changes was explained by the presence of two types of transitions, namely, macroscopic and microscopic.[54] While the latter indicates the emergence of hydrophobic associations, the former is evidenced by volume reduction and occurs when hydrophobic interactions are strong enough to overcome the swelling power caused by excess charge and hydrophilic groups.

Thick PEMUs are, in fact, not totally intrinsically compensated.[37] For the PAH/PSS control PEMU, we have measured a residual extrinsic charge of about 6%.[41] In other words, 6% of the polyelectrolyte charge is balanced by counterions. These counterions, though dilute, exhibit high osmotic pressure, causing the long-range interactions that perturb the volume transition. Interestingly, Shibayama et al.[42] report an increase of about 10 °C in the onset of volume transition for a 5% charged NIPAM gel—approximately what is observed here (Figure 4).

For the purposes of quantitative analysis, an electrostatic cross-link exists for every one PSS and one PAH unit; two NIPAM monomers; and a number of water molecules. Having the PAH/PSS control PEMU (Figure 4) allows us to assign six water molecules to each PAH/PSS ion pair, leaving about nine water molecules/2NIPAM monomers at 45 °C, as compared to one to three H_2O/NIPAM remaining after dehydration of a cross-linked NIPAM gel.[42] Continuing this "water budgeting," the multilayer loses about 13 water molecules/2NIPAM, less than the range of 10−15 H_2O/NIPAM segments lost from the cross-linked charged NIPAM gel upon transition.[42] Bae et al.[4] reported an effective cross-link density of about 9.0×10^{-5} mol cm^{-3} for NIPAM gel whereas 1.0×10^{-3} mol cm^{-3} was calculated for our multilayer system. This high degree of effective cross-linking reduces the extent of collapse and probably suppresses water loss from the multilayer at the end of volume transition.

For a better understanding of these observations, the polymer−solvent interaction parameters χ_P, $\chi_{PAH/PSS}$, χ_{NIPAM}, corresponding to an average for all polymers, the PAH/PSS part, and the NIPAM part, respectively, were calculated. The Flory−Rehner equation,[55] the method of choice to analyze swelling behavior of polymer networks, considers the chains between cross-links to be flexible and long enough so that a Gaussian chain distribution can be assumed. For highly cross-linked systems such as the present case, we make use of the Peppas−Lucht model,[56] which applies to a non-Gaussian distribution of chain lengths between cross-links.

$$\chi_P = \left[\left(\frac{1}{2}\Phi_P - {\Phi_P}^{1/3}\right)\left(1 + \frac{v^0 M_r \nu}{\lambda}{\Phi_P}^{1/3}\right)^2 - \frac{1}{v^0 V_{H_2O}}\left(1 - \frac{v^0 M_r \nu}{\lambda}{\Phi_P}^{2/3}\right)^3 (\ln(1-\Phi_P) + \Phi_P)\right] \Big/ \left[\frac{1}{v^0 V_{H_2O}}{\Phi_P}^2\left(1 - \frac{v^0 M_r \nu}{\lambda}{\Phi_P}^{2/3}\right)^3\right] \quad (1)$$

where Φ_P is the polymer repeat unit volume fraction in the swollen state (or $\Phi_{PAH/PSS}$, Φ_{NIPAM} depending on the system considered) at different temperatures. V_{H_2O}, λ, M_r, v°, and ν are the water molar volume (18 cm^3 mol^{-1}), number of links per repeating unit, molecular weight of repeating unit, cross-linking density (mol cm^{-3}), and specific volume of the polymer, respectively. Details of this calculation are found in the Supporting Information.

The polymer−solvent interaction parameter describes the change in the free energy of the system caused by the mixing process. χ values of PEMU (Figure 5), show

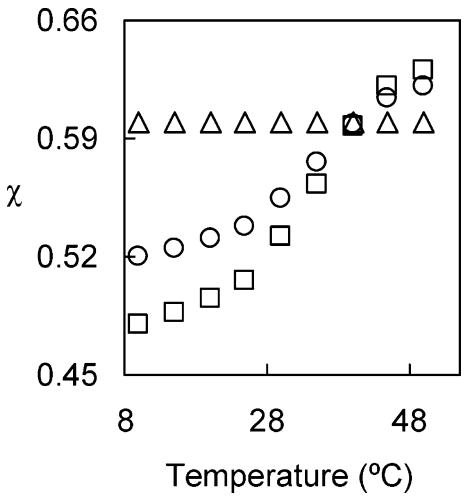

Figure 5. Variation of χ with temperature. Squares, circles, and triangles correspond to, χ_{NIPAM}, χ_P, and $\chi_{PAH/PSS}$ respectively. The values were calculated using eq 1 with $V_{H_2O} = 18$ and $v^\circ = 1.11 \times 10^{-3}$ mol cm^{-3}.

a network with a reduced degree of swelling, i.e.; poorer solvent for the polymer. The introduction of hydrated groups like NIPAM produced a network that is more thermodynamically compatible with water; thus, the degree of swelling increased, and the polymer chains approach the limits of unperturbed dimensions. As the temperature increased, χ_{NIPAM} increased from 0.48, reaching a maximum of 0.65, less than that observed in the case of cross-linked NIPAM gel where a value of >1 was reached at 55 °C.[4] This less efficient thermal response is supported by the four water molecules/NIPAM monomer left at the end of the volume transition, due to a high cross-link density compared to the NIPAM gels.[4]

The enthalpy of mixing, for the N−PEMU, can also be calculated using:

$$\chi^{h}_{NIPAM} = -T\left(\frac{\delta\chi_{NIPAM}}{\delta t}\right) \quad (2)$$

$$\Delta H_m = \mathscr{R}TN^{NIPAM}_{H_2O}\chi^{h}_{P}\Phi_P \quad (3)$$

where $N^{NIPAM}_{H_2O}$ and χ^{h}_{NIPAM} are, respectively, moles of water assigned to the NIPAM pair and the enthalpic polymer−solvent interaction parameter.

Using eqs 2 and 3, a maximum of −3.1 kJ mol^{-1} for ΔH_m was obtained at 33 °C, which is less than the range reported for cross-linked neutral NIPAM gel of −3.3 to −4.5 kJ mol^{-1}.[57] ΔH_m was observed to decrease with an increase in the mole fraction of incorporated hydrophilic monomers,[42] and this might explain the lower enthalpy value obtained for N−PEMU.

Controlling Permeation of Ions Through NIPAM Multilayers. A recent research focus has been on adapting NIPAM membranes for controlled drug release.[58−60] When the LCST is reached, the film will expel water molecules and a water-soluble probe ion will either partition less into the membrane (because of increased hydrophobicity) or its diffusion coefficient will decrease, and its release will be retarded.[61]

The ability of N−PEMUE (PAH-*co*-PNIPAM/PSS-*co*-PNIPAM)$_{18}$PAH-*co*-PNIPAM@0.2 M NaCl@pH 9 (a thinner NIPAM-containing multilayer for permeability studies, thickness 2400 Å) to influence the flux of ions was studied via RDE voltammetry[62] and compared to that of PEMUE, (PAH/PSS)$_{18}$ (PAH)@0.2 M NaCl@pH 9 (650 Å). The flux of water-soluble, electrochemically active probe ion, potassium ferricyanide through a multilayer coated electrode was monitored as a function of temperature.

In a well-stirred system such as the one used here, the stagnant aqueous layer next to the electrode is much thicker than the typical multilayer. Using limiting currents for bare electrodes, contributions to resistance to mass transfer through the stagnant film can be precisely removed from the overall mass-transfer resistance to yield the membrane-limited current, I_m, and the corresponding flux, J_m, of the probe ion[32]

$$J_m = \frac{I_m}{nFA} = \frac{\overline{DC}}{d_{(T)}} \quad (4)$$

where $\bar{D}$ and $\bar{C}$ are the respective membrane diffusion coefficient and concentration of the probe ion, $d_{(T)}$ is the multilayer thickness at different temperatures, A is the electrode area, n is the number of electrons transferred (1 in this case), and F is Faraday's constant (96 490 C mol^{-1}). To normalize for the thickness difference between N−PEMUE and PEMUE, permeability[63] (ρ, cm^2 s^{-1}) was calculated from J_m using

$$\rho = \frac{J_m d_{(T)}}{C_{sol}} = \frac{\overline{DC}}{C_{sol}} \quad (5)$$

where C_{sol} is the concentration of the probe ion in solution (moles cm^{-3}). $d_{(T)}$ was determined from the volume swelling ratio (Φ_P^{-1}),

$$d_{(T)} = \Phi_P^{-1} d \quad (6)$$

where d is the thickness of the dry multilayer measured via profilometry.

Both PEMUE and N−PEMUE bear a net positive polymer surface charge allowing negative ions to be included into the surface by the classical Donnan action.[64] Enhanced surface concentration normally leads to greater $\bar{C}$ and an appreciable flux (current) should be expected.[32,37] However, both multilayers blocked the flux of ferricyanide to an undetectable value (detection limit of 3×10^{-10} cm^2 s^{-1}) despite Donnan inclusion, revealing the passivating nature of such PAH-containing multilayers.[65]

We have recently demonstrated how the flux of charged probe ions through a multilayer is dependent on the density of extrinsic sites.[32,37] In the case of PEMU, the residual extrinsic charge fraction,[41] y_{rpe}, was found to be around 0.06 (6%) which was insufficient to promote measurable hopping transport of a triply charged ion like ferricyanide. To create more extrinsic sites, we took advantage of the pH-sensitive state of ionization of PAH (a weak polyelectrolyte). Building the multilayer at pH 9.0 and then running the experiments at pH 6.5 would create positive extrinsic sites (required for membrane transport of a negative ion) and the permeation of the probe ion would be facilitated.[63]

This strategy led to a measurable flux of ferricyanide, allowing better evaluation of the thermoresponsive behavior of NIPAM-containing multilayers. Flux across these thin multilayer membranes is governed by diffusion, a thermally activated process. The permeability of PEMUE increased as a function of temperature (Figure 6), as expected, in contrast to that of N−

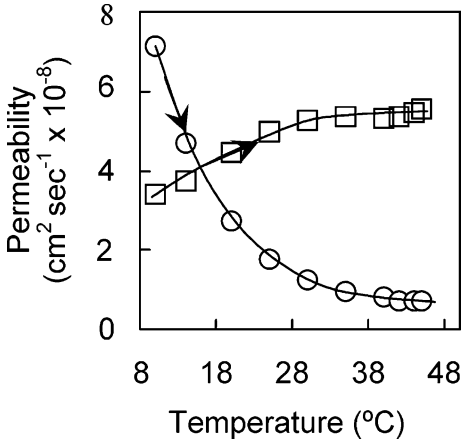

Figure 6. Membrane permeability at the rotating disk electrode as a function of temperature for PEMUE (squares) and N−PEMUE (circles). RDE experiments were run in MES buffer (0.025 M, pH 6.5, 2 M NaCl) and 1 mM $Fe(CN)_6^{-3}$.

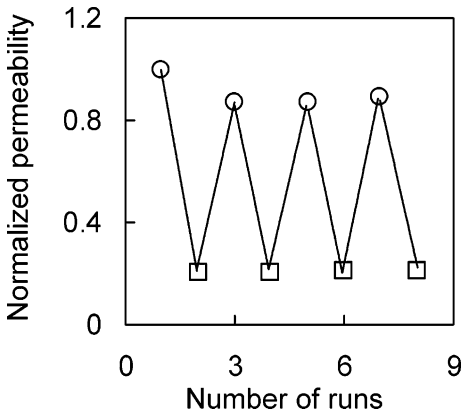

Figure 7. Permeability normalized to the first run at 10 °C as a function of temperature for N−PEMUE. Circles and squares are runs at 10 and 33 °C, respectively. RDE experiments were run in MES buffer (0.025 M, pH 6.5, 3M NaCl) and 1 mM $Fe(CN)_6^{-3}$.

PEMUE, which decreased (Figure 6). The dehydration of N−PEMUE clearly outweighs any thermal activation processes here.

Reproducibility in the thermoresponse of N−PEMUE was assessed by multiple switching between 10 and 33 °C. Figure 7 shows a reversible decrease of more than 75% in the flux at 33 °C, revealing the effectiveness of N−PEMUE in blocking the passage of ferricyanide.

Equation 5 shows that the permeability of ferricyanide depends on both $\bar{D}$ and $\bar{C}$. The concentration of the probe ion inside the thin film was measured with in situ ATR−FTIR[32] as a function of temperature using the CN stretch at 2130 cm^{-1}, and $\bar{C}$ was found to change only slightly—not enough to have an appreciable effect on permeability, leaving $\bar{D}$ as the principal parameter controlling the flux of potassium ferricyanide through N−PEMUE (see Supporting Information).

Conclusion

NIPAM containing multilayers were prepared and shown to possess thermoreversible behavior. Upon heating, about 50% of the multilayer water content was reversibly expelled. The differences in water content on temperature cycling were smaller than those for cross-linked NIPAM gels due to the greater effective cross-link density in the multilayer system. The difference in LCST estimated from amide II peak shift and water content experiments suggested the presence of two types of transitions, microscopic at 33 °C and macroscopic at 45 °C. While the former manifested as a first-order phase transition and indicates the emergence of hydrophobic associations, the latter was evidenced by volume reduction and occurs when hydrophobic interactions are strong enough to overcome the swelling power caused by excess charged and hydrophilic groups. The enthalpy of mixing at 33 °C was estimated to be −3.1 kJ mol^{-1}.

RDE experiments proved the effectiveness of the multilayer in controlling the flux of electroactive probe molecules, suppressing the flux of potassium ferricyanide by about 75% at 33 °C. The constancy of the partition coefficient of the multilayer at different temperatures was evidenced by an almost constant $\bar{C}$, indicating that $\bar{D}$ is the major parameter changing permeability.

A promising application of NIPAM multilayers is for controlled drug release. Using potassium ferricyanide as an example of a drug molecule, capsules coated with NIPAM multilayer membranes can be loaded at 20 °C ($\rho = 7 \times 10^{-8}$ cm^2 s^{-1}), and then controlled release can be achieved at body temperature with $\rho = 5 \times 10^{-9}$ cm^2 s^{-1}.

Acknowledgment. The authors are grateful to Mr. Husam Jumaa of the Department of Chemistry and Biochemistry at the Florida State University for help with copolymer characterization. This work was supported by a grant from the National Science Foundation (DMR-0309441).

Supporting Information Available: Text giving the calculation of d_p, with a figure showing the ATR−FTIR Ge crystal, text describing the in situ measurement of $\bar{C}$, with a figure showing the NPEMU1 concentration of cobalticyanide probe ion as a function of temperature, a figure showing the infrared spectra of NPEMU, text giving the calculation of the cross-linking density and the calculation of M_r, λ, and Φ_P, a figure showing the effect of temperature on flux through N−PEMUE, and text discussing the failed compositions. This material is available free of charge via the Internet at http://pubs.acs.org.

References and Notes

(1) Cho, E. C.; Lee, J.; Cho, K. *Macromolecules* **2003**, *36*, 9929.
(2) Grinberg, V. Ya.; Dubovik, A. S.; Kuznetsov, D. V.; Grinberg, N. V.; Grosberg, A. Yu.; Tanaka, T. *Macromolecules* **2000**, *33*, 8685.
(3) Schild, H. G. *Prog. Polym. Sci.* **1992**, *17*, 163.
(4) Bae, Y. H.; Okano, T.; Kim, S. W. *J. Polym. Sci., Polym. Phys. Ed.* **1990**, *28*, 923.
(5) Shibayama, M.; Tanaka, T. *Adv. Polym. Sci.* **1992**, *109*, 1.
(6) Kanazawa, H.; Kashiwase, Y.; Yamamoto, K.; Matsushima, Y.; Kikuchi, A.; Sakurai, Y.; Okano, T. *Anal. Chem.* **1997**, *69*, 823.
(7) Okano, T.; Kikuchi, A.; Sakurai, Y.; Takei, Y.; Ogata, N. *J. Controlled Release* **1995**, *36*, 125.
(8) Dong, L.; Hoffman, A. S. *J. Controlled Release* **1991**, *15*, 141.
(9) Iwata, H.; Oodate, M.; Uyama, Y.; Amemiya, H.; Ikada, Y. *J. Membr. Sci.* **1991**, *55*, 119.
(10) Kanazawa, H.; Yamamoto, K.; Matsushima, Y.; Takai, N.; Kikuchi, A.; Sakurai, Y.; Okano, T. *Anal. Chem.* **1996**, *68*, 100.
(11) Lakhiari, H.; Okano, T.; Nurdin, N.; Luthi, C.; Descouts, P.; Muller, D.; Jozefonvicz, J. *Biochim. Biophys. Acta-Gen. Subj.* **1998**, *1379*, 303.
(12) Ito, Y.; Chen, G.; Guan, Y. Q.; Imanishi, Y. *Langmuir* **1997**, *13*, 2756.
(13) Takei, Y. G.; Aoki, T.; Sanui, K.; Ogata, N.; Sakurai, Y.; Okano, T. *Biomaterials* **1995**, *16*, 667.
(14) Okano, T.; Yamada, N.; Okuhara, M.; Sakai, H.; Sakurai, Y. *Biomaterials* **1995**, *16*, 297.

(15) Von Recum, H.; Okano, T.; Kim, S. W. *J. Controlled Release* **1998**, *55*, 121.
(16) Yamato, M.; Okuhara, M.; Karikusa, F.; Kikuchi, A.; Sakurai, Y.; Okano, T. *J. Biomed. Mater. Res.* **1999**, *44*, 44.
(17) Kubota, H.; Nagaoka, N.; Katakai, R.; Yoshida, M.; Omichi, H.; Hata, Y. *J. Appl. Polym. Sci.* **1994**, *51*, 925.
(18) Peng, T.; Chen, Y. L. *J. Appl. Polym. Sci.* **1998**, *70*, 2133.
(19) Park, Y. S.; Ito, Y.; Imanishi, Y. *Langmuir* **1998**, *14*, 910.
(20) Akerman, S.; Viinikka, P.; Svarfvar, B.; Putkonen, K.; Jarvinen, K.; Kontturi, K.; Nasman, J.; Urtti, A.; Paronen, P. *Int. J. Pharm.* **1998**, *164*, 29.
(21) Lee, Y. M.; Ihm, S. Y.; Shim, J. K.; Kim, J. H.; Cho, C. S.; Sung, Y. K. *Polymer* **1995**, *36*, 81.
(22) Lee, Y. M.; Shim, J. K. *Polymer* **1997**, *38*, 1227.
(23) Okano, T.; Yamada, N.; Sakai, H.; Sakurai, Y. *J. Biomed. Mater. Res.* **1993**, *27*, 1243.
(24) Pan, Y. V.; Wesley, R. A.; Luginbuhl, R.; Denton, D. D.; Ratner, B. D. *Biomacromolecules* **2001**, *2*, 32.
(25) Decher, G. *Science* **1997**, *277*, 1232.
(26) Decher, G., Schlenoff, J. B., Eds. *Multilayer Thin Films*: *Sequential Assembly of Nanocomposite Materials*; Wiley-VCH: Weinheim, Germany, 2003.
(27) Glinel, K.; Sukhorukov, G. B.; Möhwald, H.; Khrenov, V.; Tauer, K.; *Macromol. Chem. Phys.* **2003**, *204*, 1784.
(28) Steitz, R.; Tauer, L. K.; Khrenov, V.; von Klitzing, R. *Appl. Phys. A.—Mater. Sci. Process.* **2002**, *74*, 519.
(29) Serpe, M. J.; Jones, C. D.; Lyon, L. A. *Langmuir* **2003**, *19*, 8759.
(30) Sukhishvili, S. A.; Granick, S. *Macromolecules* **2002**, *35*, 301.
(31) Kozlovskaya, V.; Ok, S.; Sousa, A.; Libera, M.; Sukhishvili, S. A. *Macromolecules* **2003**, *36*, 8590.
(32) Farhat, T. R.; Schlenoff, J. B. *J. Am. Chem. Soc.* **2003**, *125*, 4627.
(33) Bergthaller, P. U.S. Patent 4,329,441, 1982.
(34) (a) Harrick, N. J. *Internal Reflection Spectroscopy*; Interscience: New York, 1967. (b) Urban, M. W. *Attenuated Total Reflectance Spectroscopy of Polymers*; American Chemical Society: Washington, DC, 1996.
(35) PEMU (N−PEMU) and PEMUE (N−PEMUE) correspond to PAH/PSS polyelectrolyte multilayers (*N*-isopropyl acrylamide containing polyelectrolyte multilayers) used for the ATR-FTIR and electrochemistry experiments, respectively.
(36) Polyelectrolyte nomenclature: $(A/B)_x$C@y@z, where A and B correspond to the first and second polyelectrolytes in a layer pair, starting with, A. C is the outer layer (often, a "capping" layer of A), *x* is the number of layer pairs. *y* and *z* are the ionic strength and pH of the buildup solution, respectively.
(37) Farhat, T. R.; Schlenoff, J. B. *Langmuir* **2001**, *17*, 1184.
(38) Bard, A. J.; Faulkner, L. R. *Electrochemical Methods*; Wiley: New York, 2002; Chapter 8.
(39) Dubas, S. T.; Schlenoff, J. B. *Langmuir* **2001**, *17*, 7725.
(40) Sukhorukov, G. B.; Schmitt, J.; Decher, G. *Ber. Bunsen-Ges. Phys. Chem.* **1996**, *100*, 948.
(41) Jaber, J. A.; Schlenoff, J. B. Manuscript to be published.
(42) Shibayama, M.; Mizutani, S.; Nomura, S. *Macromolecules* **1996**, *29*, 2019.
(43) Hahn, M.; Gornitz, E.; Dautzenberg, H. *Macromolecules* **1998**, *31*, 5616.
(44) Deng, Y. L.; Pelton, R. *Macromolecules* **1987**, *26*, 1053.
(45) Kokufuta, E.; Zhang, Y. Q.; Tanka, T.; Mamada, A. *Macromolecules* **1993**, *20*, 1342.
(46) Urry, D. W. *Prog. Biophys. Mol. Biol.* **1992**, *57*, 23.
(47) Sasaki, S.; Kawasaki, H.; Maeda, H. *Macromolecules* **1997**, *30*, 1847.
(48) Fang, M.; Kim, C. H.; Saupe, G. B.; Kim, H.-N.; Waraksa, C. C.; Miwa, T.; Fujishima, A.; Mallouk, T. E. *Chem. Mater.* **1999**, *11*, 1526.
(49) Yoshikawa, Y.; Matsuoka, H.; Ise, N. *Br. Polym. J.* **1986**, *18*, 242.
(50) Shibayama, M.; Morimoto, M.; Nomura, S. *Macromolecules* **1994**, *27*, 5060.
(51) Yoo, M. K.; Sung, Y. K.; Lee, Y. M.; Cho, C. S. *Polymer* **2000**, *41*, 5713.
(52) Otake, K.; Inomata, H.; Konno, M.; Saito, S. *J. Chem. Phys* **1989**, *91*, 1345.
(53) Shibayama, M.; Tanaka, T.; Han, C. C. *J. Chem. Phys.* **1992**, *97*, 6829.
(54) Shibayama, M.; Tanaka, T.; Han, C. C. *J. Chem. Phys.* **1992**, *97*, 6842.
(55) Flory, P. J. *J. Chem. Phys.* **1950**, *108*, 18.
(56) Barr-Howell, B. D.; Peppas, N. A. *Polym. Bull.* **1985**, *13*, 91.
(57) Otake, K.; Inomata, H.; Konno, M.; Saito, S. *Macromolecules* **1990**, *23*, 283.
(58) Hoffman, A. S.; Afrassiabi, A.; Dong, L. C. *J. Controlled Release* **1986**, *4*, 213.
(59) Bae, Y. H.; Okano, T.; Hsu, R.; Kim, S. W. *Makromol. Chem. Rapid Commun.* **1987**, *8*, 481.
(60) Miyajima, M.; Yoshida, M.; Sato, H.; Omichi, H.; Kataki, R.; Higuchi, W. I. *Int. J. Pharm.* **1993**, *95*, 153.
(61) Kono, K.; Okabe, H.; Morimoto, K.; Takagishi, T. *J. Appl. Polym. Sci.* **2000**, *77*, 2703.
(62) Ikeda, T.; Schmehl, R.; Denisevich, P.; Willman, K.; Murray, R. W. *J. Am. Chem. Soc.* **1982**, *104*, 2683.
(63) Rmaile, H. H.; Farhat, T. R.; Schlenoff, J. B. *J. Phys. Chem. B.* **2003**, *107*, 14401.
(64) Helfferich, F. *Ion exchange*; McGraw-Hill: New York, 1962; Chapter 8.
(65) Harris, J. J.; Bruening, M. L. *Langmuir* **2000**, *16*, 2006.

MA0485235